Evaluation of the Behaviour of Reinforced Concrete Curved in-Plane Beams

Anas H. Yousifany
Building and Construction Engineering Department
University of Technology

Abstract

A full three dimensional finite element computational model is constructed for nonlinear analysis of reinforced concrete curved beams. This model was presented utilizing computer program ANSYS (Version 11), which is capable of an efficient analysis of the response at different load levels including ultimate loads.

This work deals with the structural analysis of concrete curved beams behaviour subjected to two concentrated loads. Concrete curved beams are widely used in building and bridge constructions. Some of the available experimental tests on reinforced concrete curved beams are theoretically analyzed. This covers load-deflection relationships, crack pattern and propagation of crack at different stages of load and ultimate load capacity. The reliability of the model is demonstrated by comparison with available experimental results and alternative numerical analyses which shows 4 – 8 % difference.

دراسة سلوك العتبات الخرسانية المسلحة المنحنية افقيا

انس حكمت يوسفاني، قسم هندسة البناء و الانشاءات / الجامعة التكنولوجية

الخلاصة

اقترح موديل (انموذج) حسابي ثلاثي الابعاد للتحليل اللاخطي لروافد خرسانية مسلحة محنية افقيا باستخدام طريقة العناصر المحددة وبالاعتماد على برنامج جاهز (ANSYS Software). لقد اعتمد البرنامج لحساب السلوك العام بكفاءة ودقة لمختلف مستويات التحميل ولغاية الفشل.

تضمن البحث تقييم تصرف الروافد الخرسانية المحنية افقيا والتي تمتاز بكثرة استخدامها في المنشات والجسور ، حيث تم اجراء تحليل نظري لنتائج عملية متوفرة . تم التحليل بتغطية الحمل-الهطول لسلوك المنشأ، رسم التشققات و نموها لمراحل مختلفة من التحميل و السعة القصوى للتحميل. تم التحقق من كفاءة الموديل المقترح بمقارنة مع النتائج العملية المتوفرة ولوحظ ان الاختلاف يتراوح بين ٤ – ٨%.

1. Introduction

Reinforced concrete beams curved in plane are frequently employed in structures such as highway bridges to provide a smooth traffic flow, interchanges in large urban areas, balconies of buildings and other structures. Few studies have been published on the behaviour of curved beams. The present study is, therefore, concerned with theoretical investigation on beams curved in plane.

A beam that is curved in plane and that is loaded normal to the plane of curvature is subjected to flexure, torsion, and shear. Studies pertaining to the analysis and design of horizontally curved bridges commenced somehow 40 years ago when the American Federal Highway Administration, in 1969, formed the Consortium of University Research Teams (CURT) [1]. The research efforts resulted in the initial development of working stress design criteria and tentative design specifications ASCE-AASHTO [2]. Since then a significant amount of work has been conducted to enhance the specification and to better understand the behaviour of curved girders. To accomplish

the objectives, it was deemed necessary to first conduct a comprehensive up-to-date literature search on work related to horizontally curve beams.

In 1969, Lee [3] presented the generalized stiffness matrix of a curved beam element with emphasis on the derivation of the stiffness matrix of uncoupled normal to plane loads. A curved beam element of uniform cross section was considered, notation as well as directions of positive nodal forces and displacements are taken as shown in Fig. 1. Force vectors are represented by arrows and moment vectors are represented according to right-hand rule by a double arrowhead. Generalized stiffness matrix was presented by the assemblage of matrix obtained by Martin [4] for a curved beam element with in-plane forces and the stiffness matrix of a curved beam element with normal-to-plane forces.

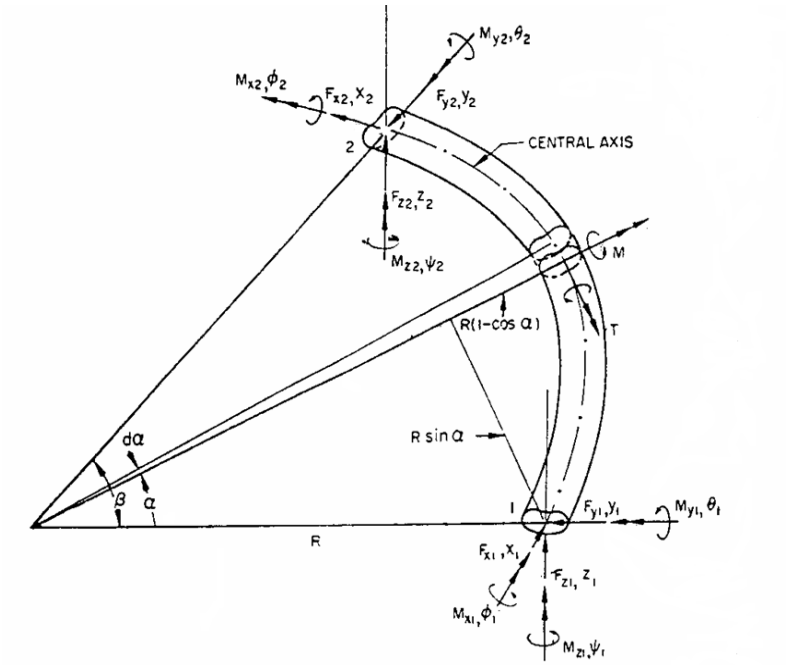

Fig. 1. Nodal forces and displacements relevant to a curved beam element [3].

In 1974, Jordaan *et al.* [5] studied the collapse of curved reinforced concrete beams. A simple plastic analysis has been used to predict the ultimate load of reinforced curved beam considering bending moment and torque only. In this method a plastic hinge is considered to be developed at a particular cross section if the following equation is satisfied.

$$\frac{M}{M_p}+\frac{T}{T_p}=1$$

where M_p is the plastic moment and T_p is the plastic torque of cross section.

Four reinforced concrete curved beams were tested; the longitudinal bars for the curved beams were cold bent to the required curvature by making a series of bends approximately 150 mm apart. In addition, six straight beams having the same cross section and reinforcement as the curved beams were tested also. Three beams were tested for each cross sectional type, bending under a single concentrated load at mid span, pure torsion and combined bending and torsion. The results of the test on the straight beams provided the basic information used for prediction of the ultimate loads of the curved beams and provided some additional support for the use of an elliptical bending-torsion interaction curve.

In 1978, Thomas *et al.* [6] studied the behaviour of reinforced concrete horizontally curved beams. They tested seven horizontally curved reinforced concrete beams fixed at both ends. The beams were subjected to a concentrated load at mid-span. The results showed that for the

conventional design of horizontally curved reinforced concrete beams it is suitable to calculate the flexure moments, torsion moments and the shear forces by an elastic analysis using the un-cracked cross section. Since moment redistribution occurs after cracking, design of curved beams using cracked section is then recommended particularly near supports where torsional moment changes rapidly along the length. For beams designed by this method the longitudinal steel yields, almost simultaneously at the supports and at mid-span. Torsional moments in a horizontally curved beam are primary moments required by equilibrium. They cannot be reduced or neglected.

In 1993, Thannon [7] proposed a full three dimensional finite element model for the nonlinear analysis of a reinforced concrete curved beam. Twenty-node isoparametric elements are used for the standard derivation of the stiffness matrix. Complete bond between the steel and the surrounding concrete was assumed. The model was used to analyze a reinforced concrete beam curved in plane and loaded by a concentrated force which was tested by Jordaan *et al* [5]. The result shows good agreement between the test and the constructed model.

2. Modelling of Material Properties

During recent years, interest in nonlinear analysis of concrete structures has increased steadily, because of the wide use of plain, reinforced and pre-stressed concrete as structural materials, and because of the development of the relatively powerful analysis techniques implemented on electronic digital computers.

The nonlinear response of concrete is caused by two major material properties, cracking in tension and plasticity in compression due to bond failure between aggregate and mortar as well as cracking of mortar itself.

In the current study, concrete material models that deal with the nonlinear three-dimensional analysis of reinforced concrete members under static increasing load are considered. These models treat the concrete as being a linear elastic-perfectly plastic-brittle-fracture material, and therefore they constitute the following:

- Stress-strain relationship model.
- Failure surface models for concrete.
- Cracking model.
- Crushing model.

These models are implemented in ANSYS program [9] and used in the present numerical investigation.

2.1 Stress-Strain Relationship

The stress-strain relations are described by elastic-perfectly plastic-brittle fracture model, as shown in Fig. 2. The concrete under a triaxial stress state is assumed to crush or crack completely once the fracture surface is reached. The complete stress-strain relationship for a perfectly plastic-brittle fracture model is developed in three parts [8]:

(1) before yielding, (2) during plastic flow, (3) after fracture.

This stress-strain relationship is expressed by a single value of Young's modulus, E, and a constant Poisson's ratio, ν. So this relation can be written in matrix form as:

$$\{\sigma\} = [D_c]\ \{\varepsilon\}$$

where:

$\{\sigma\}$= stress vector

$[D_c]$= constitutive matrix for concrete

$\{\varepsilon\}$= strain vector

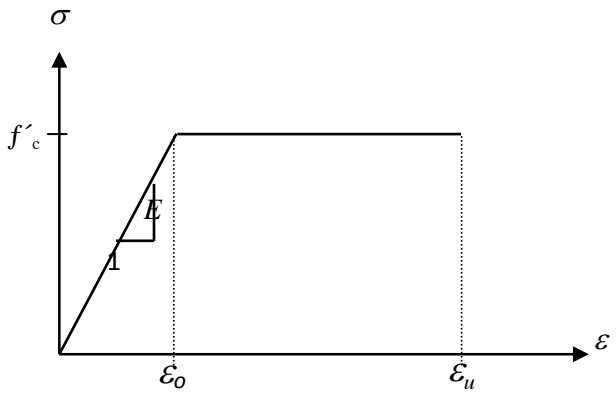

Fig. 2. Uniaxial stress-strain relationship used for concrete [8].

2.2 Failure Surface Models for Concrete

Willam and Warnke (1974) [10], developed a widely used model for the triaxial failure surface of unconfined plain concrete. The failure surface in principal stress-space is shown in Fig. 3. The mathematical model considers a sextant of the principal stress space because the stress components are ordered according to $\sigma_1 \geq \sigma_2 \geq \sigma_3$. These stress components are the major principal stresses.

The failure surface is separated into hydrostatic (change in volume) and deviatoric (change in shape) sections as shown in Fig. 4. The hydrostatic section forms a meridianal plane which contains the equisectrix $\sigma_1=\sigma_2=\sigma_3$ as an axis of revolution (see Fig. 3). The deviatoric section in Fig. 4 lies in a plane normal to the equisectrix (dashed line in Fig. 4).

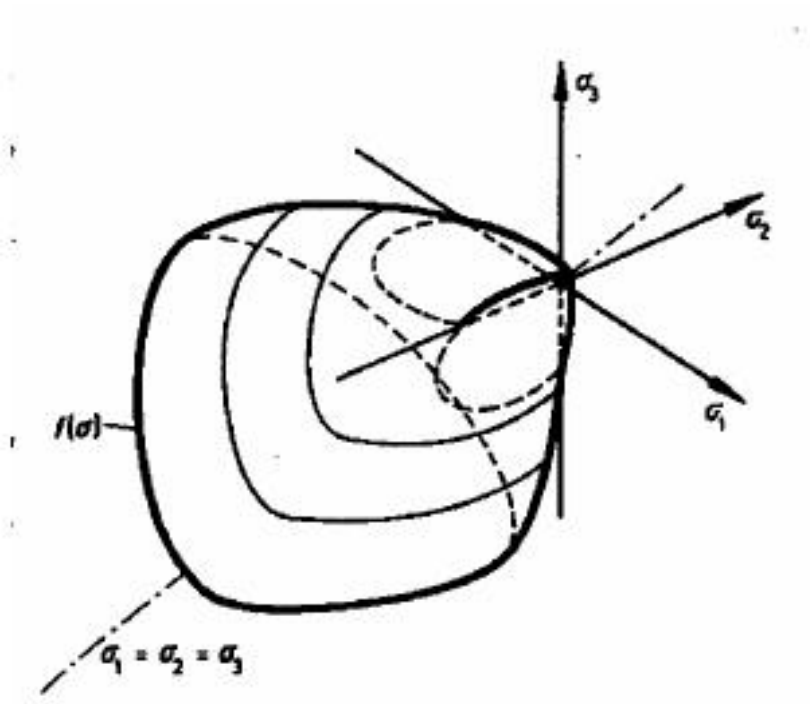

Fig. 3. Failure surface of plain concrete under triaxial conditions [10].

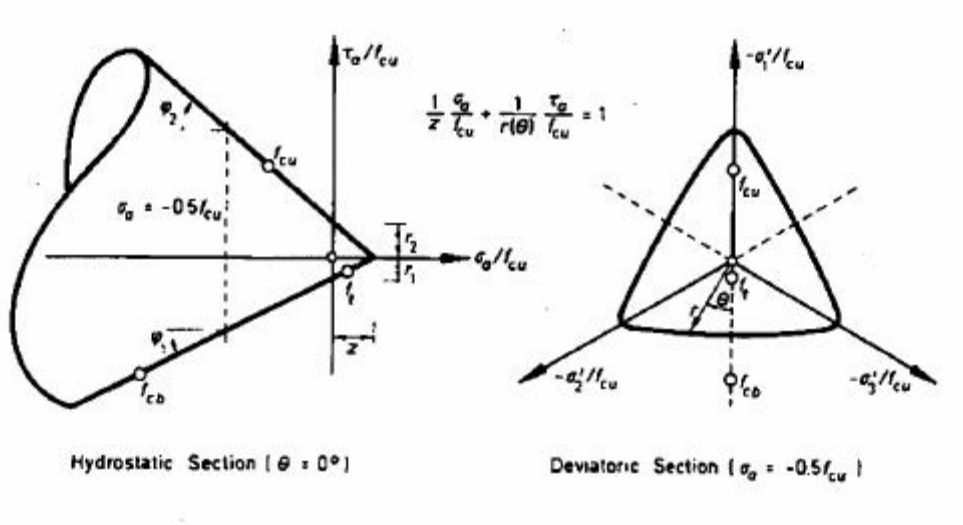

Fig. 4. Three parameter model [10].

The yield condition can be approximated by three or five parameter models distinguishing linear from non-linear and elastic from inelastic deformations using the failure envelope defined by a scalar function of stress $f(\sigma)=0$ through a flow rule, while using incremental stress-strain relations. Thus, failure surface can be expressed in terms of principal stresses and five input parameters $\left(f'_c,\ f_t,\ f_{cb},\ f_1\ and\ f_2\right)$. Where:

f'_c = ultimate uniaxial compressive strength.

f_t = ultimate uniaxial tensile strength.

f_{cb} = ultimate biaxial compressive strength.

f_1 = ultimate compressive strength for a state of biaxial compression superimposed on hydrostatic stress state.

f_2 = ultimate compressive strength for a state of uniaxial compression superimposed on hydrostatic stress state.

f'_c and f_t can be specified from two simple tests, and the other three constants can be determined from Willam and Warnke [10]:

$f_{cb} = 1.2\,f'_c$

$f_1 = 1.45\,f'_c$

$f_2 = 1.725\,f'_c$

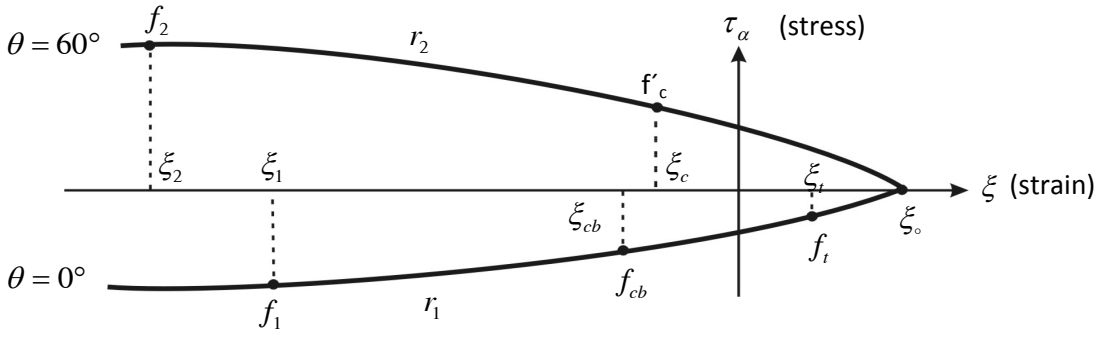

Fig. 5. Profile of the failure surface as function of five parameters [9].

In Fig. (5), the lower curve represents all stress states such that $\theta = 0°$ while the upper curve represents stress states such that $\theta = 60°$. If the failure criterion is satisfied, the material is assumed to crush.

2.3 Cracking Model

The cracked concrete is generally modelled by a linear-elastic-fracture relationship. When a principal stress exceeds its limiting value, a crack is assumed to occur in a plane normal to the direction of the offending principal stress. The cracking of concrete in the present study is modelled as "smeared-cracking model", as shown in Fig. 6.

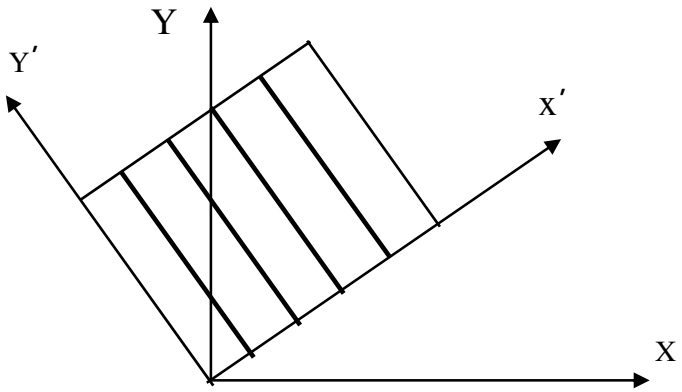

Fig. 6. Smeared crack modelling [11].

2.3.1 Post Cracking Model

The tensile stress normal to the crack dose not drop to zero immediately when the crack is formed, it decreases with increasing crack width. The tensile stress normal to the cracked plane is gradually released, and represented by an average stress-strain curve [9], as shown in Fig. 7.

For $\varepsilon_c^{cr} \le \varepsilon_n \le \alpha_1 \varepsilon_c^{cr}$ then $\sigma_n = \alpha_2 \cdot \sigma_{cr} \dfrac{\left[\alpha_1 - \dfrac{\varepsilon_n}{\varepsilon_c^{cr}}\right]}{[\alpha_1 - 1.0]}$

For $\varepsilon_n > \alpha_1 \varepsilon_c^{cr}$ then $\sigma_n = 0$

Where σ_n and ε_n are the stress and strain normal to the cracked plane, ε_c^{cr} is the cracking strain associated with cracking stress σ_{cr} equal to f_t and α_1 and α_2 are the tension stiffening parameters. α_1 represents the rate of stress release as the crack widens, while α_2 represents the sudden loss of stress at instant of cracking.

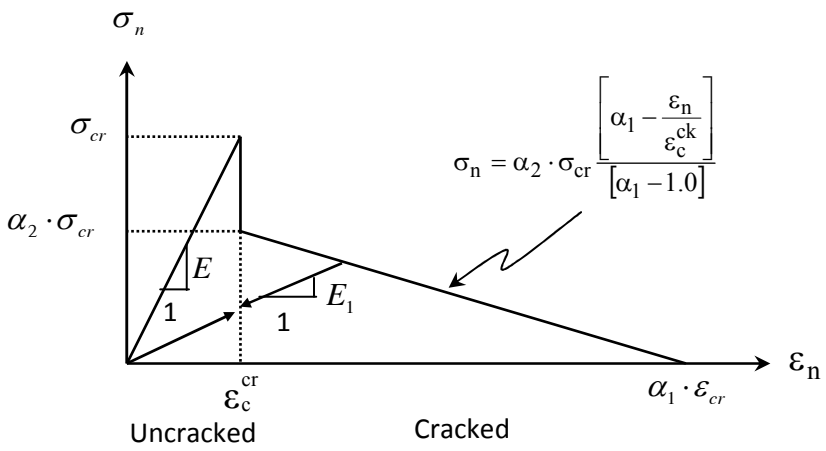

Fig. 7. Post-cracking model for concrete [9].

2.4 Crushing Model

If the material at an integration point (the sampling points for stresses and material state determination [9]) fails in uniaxial, biaxial or triaxial compression, the material is assumed to crush at that point. Under this condition, the material strength is assumed to have degraded to an extent such that the contribution to the stiffness of an element at the integration points in question can be ignored [9].

3. Modelling of Reinforcing Bars

Since steel reinforcement elements are mostly one-dimensional, transmit axial force only and relatively slender, the stress-strain behaviour can be assumed to be identical in tension and compression. In the current study, a bilinear isotropic uniaxial stress-strain relationship is used for steel reinforcement as shown in Fig. 8.

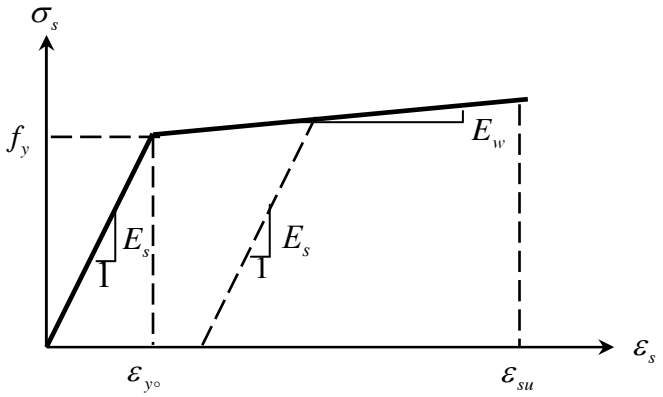

Fig. 8. Stress – strain relationship of steel bar [12].

Where E_s is modulus of elasticity of steel, E_w is hardening modulus of elasticity of steel (Tangent modulus) and can be calculated as a ratio of (0.02 E_s – 0.03 E_s), f_y is the yield strength of reinforcing bars, ε_{yo} is the initial yield strain of steel, and ε_{su} is the ultimate strain of steel.

4. ANSYS Finite Element Model

In the current study, three-dimensional 8-node (solid 65) elements are used to model the concrete [9]. This element has eight corner nodes, and each node has three degrees of freedom "*u*, *v* and *w*" in the "*x*, *y* and *z*" directions respectively. The element is capable of plastic deformation, cracking in three orthogonal directions, and crushing. "Solid 65" element has one solid material (concrete) and up to three rebar reinforcements in three orthogonal directions, as shown in Fig. 9.

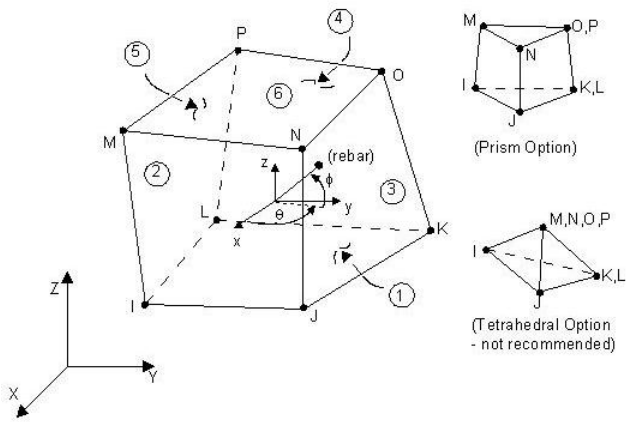

Fig. 9. Solid 65 element [9].

The reinforcement is included within the properties of the 8-node brick elements (smeared model) to include the reinforcement effect in the concrete structures. The reinforcement is assumed to be capable of transmitting axial forces only, and a perfect bond is assumed to exist between the concrete and the reinforcing bars.

4.1 Case Study

Two reinforced concrete curved beams (C3 and C4) which have been tested by Jordaan [5] are chosen for analysis to discuss the ability of using the finite element model utilizing experimental load-deflection behaviour. The beams were loaded by two equal concentrated load, their geometry, cross section, and the position of applied load are shown in Fig. 10.

Material properties are given in Table 1 and the reinforcement details are given in Table 2. The boundary conditions at the supports are kept fixed. This fixity is maintained during the test to produce zero rotation. The finite element idealization is shown if Fig. 11.

In Figs. 12. a and 12. b the experimental load deflection curves at mid-span section of beams C3 and C4 is compared with the curves predicted using the present model. The results show a good agreement with the test results. The ultimate loads from experiment are compared in Table 3 with the present results. The good agreement of the present analysis with experiment is obvious.

ANSYS program is capable of recording a crack pattern at each applied load step. Figure 13 shows evolutions of crack patterns developing for beam C3 at selected stages of applied load.

Table 1. Material Properties of Jordaan's Beams [5].

Young's Modulus of Steel E_s = 200000 MPa
Young's Modulus of Concrete E_c =16660 MPa
Concrete Compressive Strength f'c = 41 MPa
Concrete Tensile Strength ft = 2.7 MPa
Concrete Poisson's Ratio ν = 0.2
Steel Poisson's Ratio ν = 0.3

Table 2. Reinforcement Details [5].

Beam designation	Longitudinal reinforcement and Yield stress	Transverse reinforcement and Yield stress	Cover over main reinforcement
C3	4ϕ22mm 384 MPa	ϕ6mm @ 100mm c/c 240 MPa	27 mm
C4	4ϕ16mm 486 MPa	ϕ10mm @ 89mm c/c 485 MPa	35 mm

Table 3. Comparison of the Ultimate Loads.

Beam designation	Experimental results [5]	Present Study	P.S. / Exp.
C3	178 kN	172 kN	0.966
C4	157 kN	145 kN	0.923

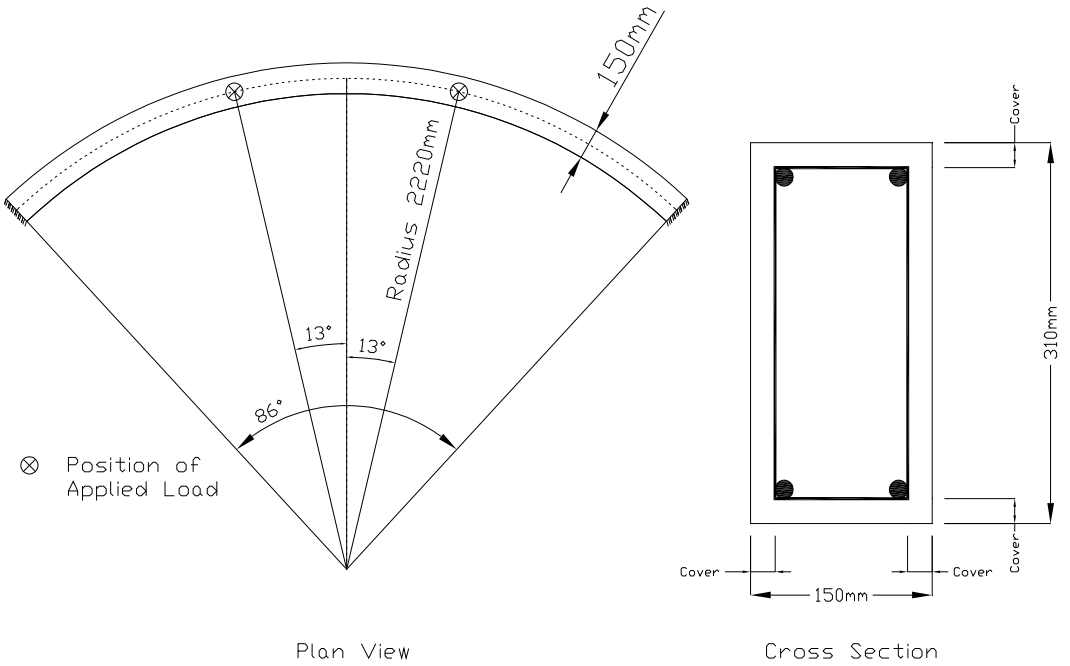

Fig. 10. Jordaan's Curved Beam, Geometry and Details [9].

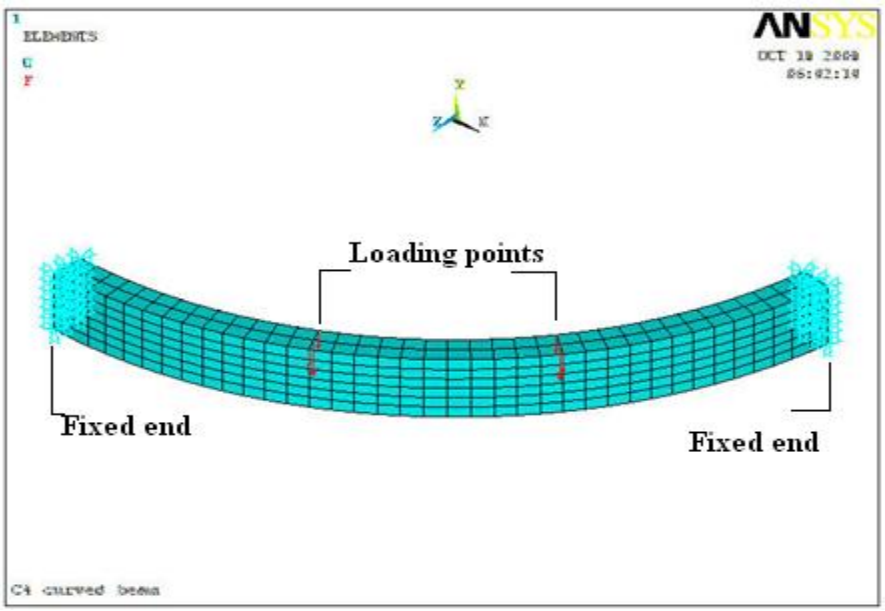

Fig. 11. Finite Element Idealization.

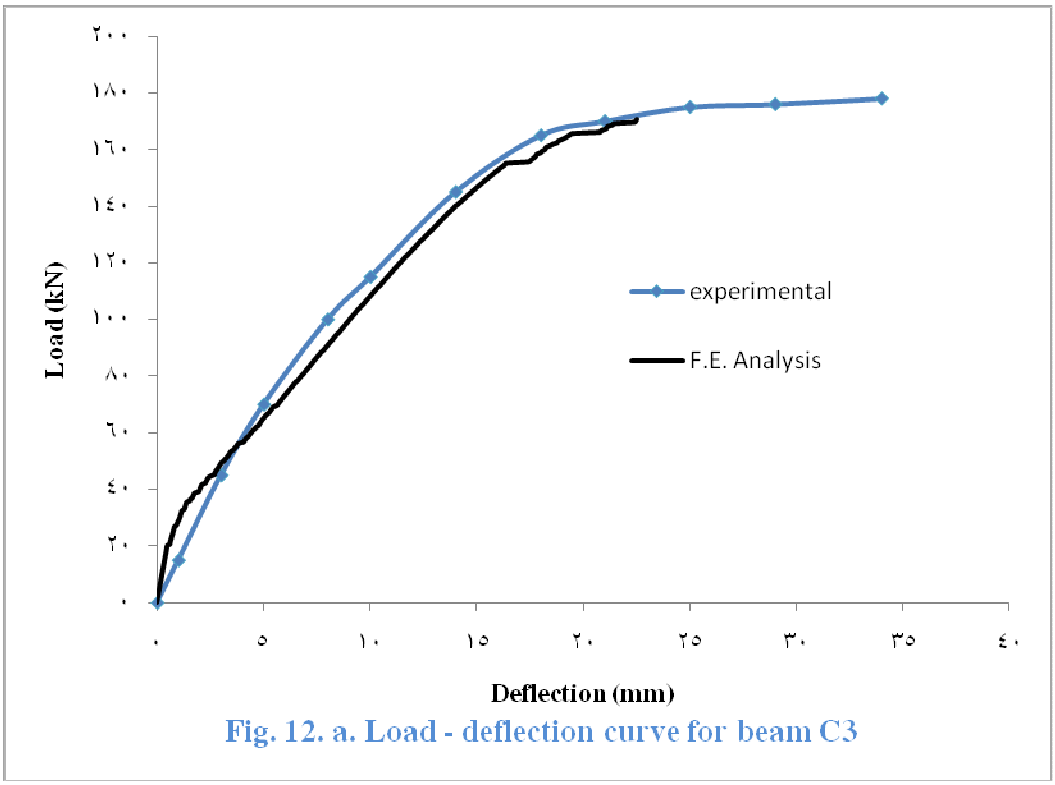

Fig. 12. a. Load - deflection curve for beam C3

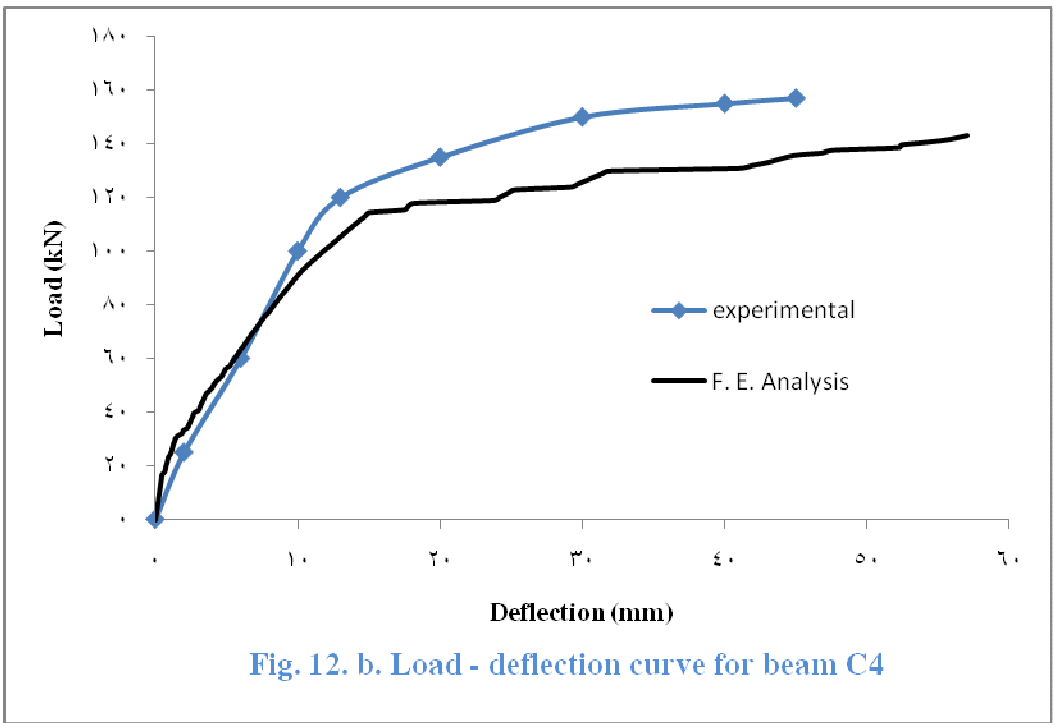

Fig. 12. b. Load - deflection curve for beam C4

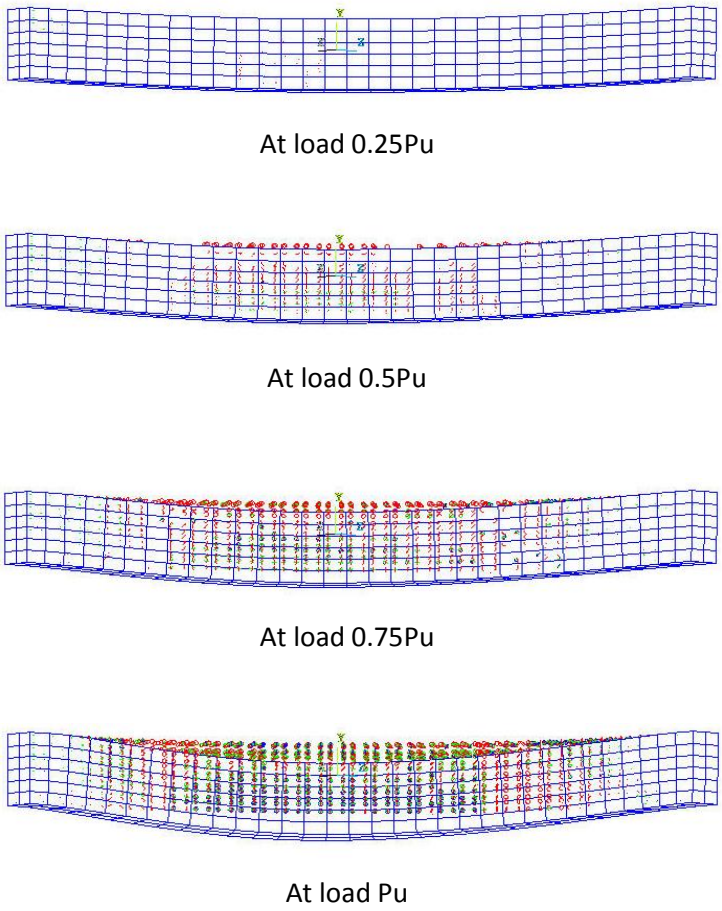

Fig. 13. Crack pattern of beam C3 carried out by ANSYS for different stages of loading.

5. Conclusions

Finite element modelling of reinforced concrete curved in-plane beams is presented in this paper. The nonlinear behaviour of curved beams has been studied with reference to those beams tested earlier by Jordaan, *et al* [5]. The software package ANSYS was employed in the analysis.

Load-deflection curves, crack patterns and ultimate load capacities were obtained from the finite element analysis. These results have been compared with the corresponding results obtained from the experiments. A close agreement between the finite element and experimental results has been observed.

The deviation in the prediction of ultimate load has been found to be 4-8% and the results established the validity of the proposed finite element model. In addition, finite element method provides extensive information on the behaviour of these beams up to failure.

7. References

1. Zurcick, A. and Naqib, B., "Horizontally curved steel I-girder state-of-art analysis methods", ASCE, *Journal of Bridge Engineering*, Vol. 4, No. 1, Feb. 1999, pp. 38-47.
2. AASHTO (1993), *"Guide Specification for Horizontally Curved Highway Bridge"*, Washington, D.C. 224 pp.

3. Lee, H. P., "Generalized stiffness matrix of curved beam element", AIAA *Journal*, Vol. 7, October 1969, pp. 2043-2045.
4. Martin, H. C., *"Introduction to Stiffness Matrix Methods of Structural Analysis"*, Mc-Graw Hill, New York, 1966, pp. 144-148.
5. Jordaan, J., Magdi, M. A. K., and McMullen, A. E., "Collapse of curved reinforced concrete beams", ASCE, *Journal of Structural Engineering*, Vol. 100, No. 11, Nov. 1974, pp. 2255-2269.
6. Thomas, T. C. Leonard, F. and Mehmet, J., "Behaviour of reinforced concrete horizontally curved beams", ACI, Vol. 75, No. 4, April 1978, pp. 112-123.
7. Thannon, A. Y., "Nonlinear three dimensional finite element analysis of reinforced concrete curved beams", *Al-Rafidain Engineering*, Vol. 1, No. 2, Feb. 1993, pp. 2-16.
8. Chen, W., *"Plasticity In Reinforced Concrete"*, McGraw-Hill Book Company, U.S.A., pp. 592, 1982.
9. Swanson Analysis System, *"ANSYS"*, Online manual, version 11 software and theory reference, U.S.A., 2007.
10. Willam, K. and Warnke, E., "Constitutive Model for the Triaxial Behaviour of Concrete", Proceedings, *International Association for Bridge and Structural Engineering*, Vol. 19, ISMES, pp. 174, Bergamo, Italy, 1975.
11. Chen, W. and Saleeb, A., *"Constitutive Equations for Engineering Materials"*, John Wiley & Sons, 1982.
12. Al- Manasser, A. and Phillips, D., "Numerical Study of Some Post-Cracking Material Parameters Affecting Nonlinear Solutions in Reinforced Concrete Deep Beams", *Canadian Journal of Civil Engineering*, Vol. 14, pp. 655 – 666, April 1987.